Biochimica et Biophysica Acta 1838 (2014) 355–363

Contents lists available at ScienceDirect

Biochimica et Biophysica Acta

journal homepage: www.elsevier.com/locate/bbamem

# Treatment of influenza virus with Beta-propiolactone alters viral membrane fusion

Pierre Bonnafous [a,b], Marie-Claire Nicolaï [c], Jean-Christophe Taveau [a,b], Michel Chevalier [c], Fabienne Barrière [c], Julie Medina [c], Olivier Le Bihan [a,b], Olivier Adam [c], Frédéric Ronzon [c], Olivier Lambert [a,b,*]

[a] University of Bordeaux, CBMN UMR 5248, IPB, IECB, F-33600 Pessac, France
[b] CNRS, CBMN UMR 5248, F-33600 Pessac, France
[c] Sanofi Pasteur, 1541 Avenue Marcel Mérieux, 69280 Marcy l'Etoile, France

ARTICLE INFO

*Article history:*
Received 29 May 2013
Received in revised form 25 September 2013
Accepted 30 September 2013
Available online 16 October 2013

*Keywords:*
Membrane fusion
Influenza virus
Beta-propiolactone
Cryo electron microscopy
Cryo electron tomography
Hemagglutinin

ABSTRACT

Beta-propiolactone (BPL) is commonly used as an inactivating reagent to produce viral vaccines. Although BPL has been described to chemically modify nucleic acids, its effect on viral proteins, potentially affecting viral infectivity, remains poorly studied. Here, a H3N2 strain of influenza virus was submitted to treatment with various BPL concentrations (2–1000 μM). Cell infectivity was progressively reduced and entirely abolished at 1 mM BPL. Virus fusion with endosome being a critical step in virus infection, we analyzed its ability to fuse with lipid membrane after BPL treatment. By monitoring calcein leakage from liposomes fusing with the virus, we measured a decrease of membrane fusion in a BPL dose-dependent manner that correlates with the loss of infectivity. These data were complemented with cryo transmission electron microscopy (cryoTEM) and cryo electron tomography (cryoET) studies of native and modified viruses. In addition, a decrease of leakage irrespective of BPL concentration was measured suggesting that the insertion of HA2 fusion peptide into the target membrane was inhibited even at low BPL concentrations. Interestingly, mass spectrometry revealed that HA2 and M1 matrix proteins had been modified. Furthermore, fusion activity was partially restored by the protonophore monensin as confirmed by cryoTEM and cryoET. Moreover, exposure to amantadine, an inhibitor of M2 channel, did not alter membrane fusion activity of 1 mM BPL treated virus. Taken together these results show that BPL treatment inhibits membrane fusion, likely by altering function of proteins involved in the fusion process, shedding new light on the effect of BPL on influenza virus.



## 1. Introduction

Infections with influenza viruses cause recurrent epidemics and global pandemics. Seasonal infection is estimated to cause between 250,000 and 500,000 deaths. Moreover, the 2009 pandemic was responsible for more than 250,000 deaths. In addition, these outbreaks have major economic consequences in terms of absenteeism, treatment and hospitalization costs. In the USA alone, this loss is estimated to be about $27 billion per year. The high capability of antigenic shift leads to the emergence of novel viruses, against which acquired immunity by previous influenza infection or vaccination is poorly efficient. Biotechnological improvements relying on genetic, structural, functional and chemical studies are required for the development of better viral treatments and more efficient vaccines to fight against present and future influenza virus variants.

The main targets of the influenza virus are epithelial cells of the respiratory tract. The outer surface of the virus [1] exposes the trimeric transmembrane glycoprotein hemagglutinin (HA) required for viral binding to sialic acid moieties on the surface of host cells [2] which initiates membrane fusion (for reviews, see [3–6]).

Each monomer of HA consists of two disulfide-linked subunits, HA1 and HA2. HA2 contains a transmembrane domain at its C-terminus side and at its N-terminus, the "fusion peptide," an amphiphilic stretch of amino acids which is buried in the HA stem at neutral pH [7]. HA1 monomers contain at the membrane-distal tip of the trimer, a receptor binding pocket composed of highly conserved amino acids (Tyr98, Ser136, Trp153 and His183) that bind sialic acid moieties *via* hydrophobic interactions or hydrogen bonds [2,8]. Once the cell membrane and the virus have been closely juxtaposed by virus–receptor interaction, the complex is internalized by endocytosis through a clathrin dependent pathway. Upon acidification of the interior of the endosome, the viral HA undergoes irreversible conformational rearrangements involving extrusion of the fusion peptide from the HA stem [9] toward the target endosomal membrane [10–13], and transformation of the HA loop region into a large coiled coil domain [9] triggering apposition and fusion of viral and endosomal membranes [12,14,15]. As a consequence of viral interior acidification arising from $H^+$ transport through the M2 channel, the viral Ribo-Nucleo-Protein complexes (vRNPs) dissociate from M1 matrix

* Corresponding author at: CBMN, UMR CNRS 5248, Université Bordeaux, Institut Polytechnique Bordeaux, Allée Geoffroy Saint-Hilaire 33600 Pessac, France. Tel.: +33 540006829, +33 540002200.
*E-mail address:* o.lambert@cbmn.u-bordeaux.fr (O. Lambert).

0005-2736/$ – see front matter © 2013 Elsevier B.V. All rights reserved.
http://dx.doi.org/10.1016/j.bbamem.2013.09.021

proteins and escape from endosome after the membrane merger. The vRNPs are then imported into the nucleus for transcription, translation and finally virus amplification [16,17].

Currently, two forms of influenza vaccine are available for widespread distribution: inactivated vaccines and live-attenuated vaccines. Preparation of inactivated vaccines consists of several steps: (i) virus of a chosen subtype is propagated in embryonated chicken eggs, (ii) the virus is purified (iii), inactivated with formaldehyde or beta-propiolactone (BPL), (iv) the inactivating reagents are removed and (v) the virus is split with detergent. To prepare the vaccine, various subtypes of influenza A (H3N2 and H1N1) as well as influenza B are then mixed to provide a broader range of protection against seasonal circulating viruses. Interestingly, the choice of virus inactivation procedure is then of great importance to effectively protect against infection. Indeed a recent report showed that whole inactivated influenza virus with beta-propiolactone (BPL) provided a better protection against different virus subtypes than split or formaldehyde-inactivated virus [18].

BPL is widely used for the inactivation of infectious agents (bacteria, fungi, viruses) in many vaccine preparations as well as in disinfection, plasma sterilization and tissue transplants [19–23]. This very widespread industrial use of BPL contrasts somehow with the limited knowledge available on the molecular consequences of its action. BPL reacts with nucleophilic reagents (including nucleic acids and proteins) leading to alkylated and/or acylated products. BPL is very reactive with different chemical moieties of various biological molecule including proteins (mostly methionine, cysteine and histidine) and nucleic acids (mainly adenosine, cytidine and guanosine moieties of the vRNA) [24–26]. BPL alters the capability of DNA to be used as template by polymerase [22]. From literature, the effect of BPL is dose and specimen -dependent. In the presence of 2 mM BPL infectivity of plasmid pUC18 is reduced while no effect was observed at 250 μM BPL [22]. At 250 μM, BPL drastically inhibits the infectious activity of phage M13 [22]. BPL seems to be more effective in inactivating enveloped viruses than non-enveloped viruses [23]. Interestingly, BPL use appears also suitable to obtain a specific immunity against respiratory syncytial virus and H5N1 virus [18,27]. BPL treatment then mediates a loss of infectivity while maintaining antigenicity. This effect has been obtained for high BPL doses more than several millimolars. These results are promising for the use of BPL in vaccine preparation. However regarding WHO and European Pharmacopoeia recommendations, a better fine-tuning of BPL doses is required for industrial vaccine production processes to assure viral inactivation.

There is a limited understanding of the relation between molecular modification and loss of infectious titer as well as the capacity of BPL to modify proteins. That limits the BPL use for preparing safe vaccines. This lack of knowledge is likely at the origin of “over inactivation” and inappropriate reaction.

In the present work, we aimed at establishing the effects of viral BPL treatment at a molecular level and thus to close this existing gap of knowledge and to study in particular the effect of this inactivating agent on viral proteins. Virus samples of the H3N2 strain were submitted to various doses of BPL. This strain is part of the seasonal influenza virus produced at industrial scale. In addition, the BPL inactivation procedure employed in this study is identical to that used to produce the commercial vaccine. The infectivity of BPL-treated virus was found to be reduced in a BPL dose-dependent manner. By combining fluorescence spectroscopy, mass spectrometry, cryo transmission electron microscopy (cryoTEM), and cryo electron tomography (cryoET), we observed that BPL-treated viruses had lost their capacity to fuse with liposomes in dose dependent manner.

## 2. Materials and methods

### 2.1. Chemical products

Egg phosphatidylcholine, *N*-(lissamine rhodamine B sulfonyl)-phosphatidylethanolamine (*N*-Rh-PE) *N*-(7-nitro-2,1,3-benzoxadiazol-4-yl)-phosphatidylethanolamine (*N*-NBD-PE) and GM3 gangliosides were purchased from Avanti Polar Lipids Inc. (Alabaster, Al), monensin from Calbiochem, cholesterol, Porcine trypsin, and amantadine from Sigma-Aldrich (St Louis, MO).

Ultrapure water with a nominal resistance of 18 mΩ cm (Milli-Q, Millipore) was used for all buffers and solutions. All other chemicals were purchased of the highest purity available from Sigma-Aldrich.

### 2.2. Liposome preparation

Multilamellar vesicles (MLV) were produced by resuspension of dry lipid films of egg phosphatidylcholine, cholesterol, ganglioside GM3 at a molar ration of 8:1:1 in a buffer A (150 mM NaCl, 5 mM HEPES pH 7.4, 1 mM EGTA). The MLV suspension was then quickly frozen in liquid nitrogen and thawed (water at 37 °C) five times. MLV suspension was then forced through 0.1 μm defined pore polycarbonate filters (Whatmann) using a manual extruder (Avanti Polar lipids) to form large unilamellar vesicles. Phospholipid phosphate concentration was determined according to Böttcher et al. [28].

### 2.3. Influenza virus preparation and BPL inactivation

An egg-grown influenza virus preparation (A/Victoria/210/2009 — H3N2) was obtained from clarified allantoic fluid and purified on a sucrose gradient. All virus work was carried out at 4 °C. Viral preparations were dialyzed over night into phosphate buffer saline (PBS) at pH 7.5 and protein concentrations determined using Bradford protein reagent (BioRad) was adjusted to 2 mg/mL. Four viral preparations were inactivated using different BPL concentrations [22,23,29,30]. In brief, sodium phosphate at a final concentration of 100 mM was added to prevent pH changes that occur with the addition of the desired (2, 20, 250 and, 1000 μM) BPL concentration. Samples were incubated with gentle stirring overnight at 4 °C. Preparations were then again dialyzed 24 hours against PBS at 4 °C. The viral protein concentration was again determined prior to conducting further experiments. Samples were stored at 4 °C with 0.01% (*w*/*v*) sodium azide and used within two months.

### 2.4. $TCID_{50}$ assay

MDCK cells were seeded in 96 well plates at a density of $3.75 \times 10^4$ cells/well in DMEM (Gibco®) supplemented with 1 μg/mL porcine trypsin. Cells were infected with 50 μL of tenfold serial dilutions of virus and incubated for 4 days, at 37 °C. Supernatants from these cultures were then tested in a hemagglutination assay. $TCID_{50}$ titers were calculated according to the method of Spearman–Karber [31].

### 2.5. Hemagglutination assay

The HA hemagglutination assay was performed by serially diluting 50 μL of culture supernatants 2-fold with PBS in V-bottom plates. Subsequently, 50 μL of 0.5% chicken red blood cells (Sanofi Pasteur, Alba-la-Romaine, France) were added to each well. The plates were incubated for 1 h at 4 °C and the hemagglutination or the absence of hemagglutination was determined visually for each well.

### 2.6. SDS-PAGE and mass spectrometry analysis

1 mM BPL-treated virus (15 μg proteins) were deglycosylated with PNGase F, denatured in XT sample buffer (Bio-Rad) under reducing conditions, and separated on a Criterion XT 4–12% Bis-Tris gel (BioRad) in MOPS-XT buffer. The gel was fixed in 50% (*v*/*v*) methanol, 7% (*v*/*v*) acetic acid for 30 min and stained using GelCode. The gel was rinsed in distilled water. Excised gel bands of interest were washed alternatively with 50 mM ammonium bicarbonate pH 8.0 and acetonitrile. Proteins were then reduced with 10 mM DTT, alkylated with 55 mM

iodoacetamide and then digested overnight with trypsin (Promega, USA) at 0.01 mg/ml diluted in ammonium bicarbonate 25 mM buffer. Digestion was not stopped by 0.1% TFA. Samples were then deposited on a matrix layer of α-cyano-4-hydroxycinnamic acid (HCCA) saturated solution in 50% acetonitrile and 0.1% TFA. Analyses were performed on an Ultraflextrem MALDI-TOF-TOF mass spectrometer in reflectron positive mode (Bruker Daltonics, Billerica, MA). External calibration was done using peptide calibrants (Bruker Daltonics, reference 222570). Mass spectra were acquired using sets of instrument parameters over the *m/z* 300 to 5000. MS/MS analysis was performed on peptides of interest. Spectra analysis was performed with FlexAnalysis and Biotools softwares.

### 2.7. Membrane fusion measurements

Membrane fusion between virus and labeled liposomes was performed with a Förster Resonance Energy Transfer (FRET) assay [32]. Labeled liposomes, prepared as described above, from a lipid film containing 0.6 mol% each of *N*-Rh-PE and *N*-NBD-PE. Fusion was measured at room temperature in buffer B (135 mM NaCl, 15 mM sodium citrate, 10 mM MES, 5 mM HEPES, 1 mM EGTA at pH 5.1) at excitation and emission wavelengths of 465 and 530 nm, respectively. For calibration of the fluorescence scale, the initial residual fluorescence intensity was set to zero and the intensity at infinite probe solution 100%. The latter value was obtained after lysis of the liposomes with Triton X-100 (0.5% *v/v*) with correction for the quenching of NBD by Triton X-100 [33]. Concentrations for liposome and virus correspond to their lipid concentrations which were 2.5 μM and 5 μM respectively and calculated as follows. For liposome, lipid concentration was estimated from phosphorus determination as detailed in liposome preparation section. For virus, lipid concentration was estimated from the Bradford determination using the lipid to protein ratio equal to 0.5 and a lipid MW of 800 Da. Membrane fusion kinetics in the presence of amantadine and monensin were monitored at 37 °C [34,35]. Before measurement, virus was incubated at room temperature for 30 min with either 1 μM of monensin (final concentration) 10, and 50 μg/mL of amantadine (final concentration). Because conformational changes of HA are faster at 37 °C than at room temperature, liposomes and virus concentrations were 7.5 μM and 15 μM respectively. For cryoTEM observations of the "monensin experiments," viruses and liposomes were incubated 3 minutes at 37 °C at pH 5.1 before vitrification.

### 2.8. Leakage measurements

Calcein encapsulating liposomes were prepared as described previously [12]. Briefly, calcein was entrapped into liposomes by hydrating the dry lipid film in isotonic buffer containing 75 mM calcein. After extrusion as described above, free dye was removed by molecular sieve chromatography on Sephadex G75 with buffer A. An increase in calcein fluorescence by dilution of self-quenched fluorescent dye due to fusion or direct leakage from liposomes was assessed by monitoring calcein fluorescence at 515 nm with excitation at 485 nm on a Perkin-Elmer LS55 spectrofluorimeter. These measurements were carried out at room temperature in buffer B. Data were normalized by setting initial fluorescence intensity of calcein-loaded liposomes to zero and the intensity of full dequenched calcein (obtained after lysis of LUV with triton X100-0.5% *v/v*) to 100. Liposomes and virus concentrations were respectively 2.5 μM and 5 μM.

### 2.9. CryoTEM and CryoET

A 5 μL sample was deposited onto a lacey carbon cupper grid (Ted pella) placed in the automated device for plunge-freezing (EM GP Leica) enabling a perfect control of temperature and relative humidity for experiment performed at 25 or 37 °C respectively. The excess of sample was blotted with filter paper and the grid was plunged into a liquid ethane bath cooled and maintained at −183 °C with liquid nitrogen. Specimens were maintained at a temperature of approximately −170 °C, using a cryo holder (Gatan, CA, USA) and observed with a FEI Tecnai F20 electron microscope operating at 200 kV and at a nominal magnification of 29,000× under low-dose conditions. Images were recorded with a 2 k × 2 k USC 1000 slow-scan CCD camera (Gatan).

For cryoET, tilt-series were collected automatically on FEI Tecnai F20 from −60° to +60° with 1° angular increment at a nominal 8 μm defocus using the UCSF tomography software [36]. Images were recorded on CCD camera with a 3.7 Å pixel size at the specimen level. Alignments of tilt series binned by a factor of two were performed with the IMOD software [37] using 10 nm colloidal gold particles as fiducial markers. Tomographic reconstructions were calculated by weighted back-projection using Priism/IVE package [38]. Final voxel size was 7.4 Å. Semi-automatic segmentation of Fig. 3C was carried out by applying one cycle of median 6 × 6 × 6 filter, a background subtract, and a threshold according to the Otsu scheme using ImageJ (Rasband, W.S., ImageJ, U. S. National Institutes of Health, Bethesda, Maryland, USA, http://rsb.info.nih.gov/ij/, 1997–2009). Tomogram rendering was calculated with the UCSF Chimera package from Resource for Biocomputing, Visualization, and Informatics at the University of California, San Francisco (supported by NIH P41 RR001081) [39].

## 3. Results

### 3.1. BPL treatment reduced irreversibly viral infectivity on host cells

The infectivity of viral samples previously treated with different concentrations (2, 20, 250 or 1,000 μM) of BPL was measured in cell culture (Fig. 1). Viruses treated with 2 μM BPL lost about 50% of their cell infectivity compared to native virus. With higher doses (10- and 125-fold), viruses lost their infectivity almost completely and treatment with 1 mM BPL caused complete suppression of infectivity. The ID50 (effective BPL dose) was estimated at 3 μM in a 95% confidence limit. Moreover, a comparable loss of infectivity was measured for inactivated viruses stored at 4 °C for two and seven months after inactivation indicating that the BPL effect was irreversible over this period of time (data not shown). In addition H1N1 influenza virus (A/Brisbane/59/2007 genotype) submitted to the same doses of BPL exhibited a similar loss of infectivity as the H3N2 virus suggesting comparable sensitivities of different viral strains to BPL treatment (Fig. S1).

### 3.2. Viral membrane fusion inhibited by BPL treatment

A crucial step in the infection process is membrane fusion with endosome. We studied the membrane fusion activity of various BPL-treated viruses with liposomes at low pH using a FRET assay according to a well established protocol [40]. Results of treated and native viruses

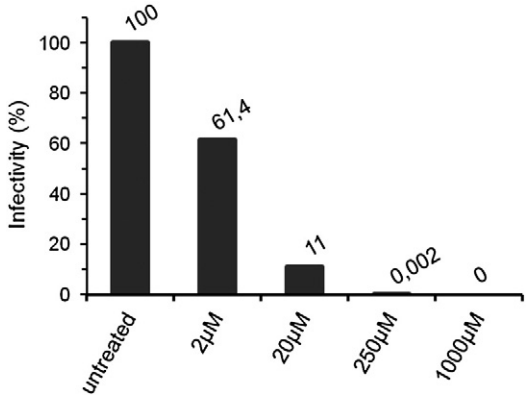


**Fig. 1.** Infectivity of A/Victoria/210/2009 (H3N2) influenza virus after treatment with various concentrations of BPL, i.e., 2, 20, 250 and 1000 μM. 100% infectivity represents native virus.

are presented in Fig. 2A. For native virus, membrane fusion activity was found to level off after approximately 12 minutes corresponding to about 45% increase in fluorescence. This level of FRET was in good agreement with results previously obtained on comparable H3N2 strain [12]. The membrane fusion activity decreased steadily with increasing BPL concentration. Both the final level and the initial rate of fusion were lowered suggesting that the number of fusion events is reduced and also that the fusion mechanism is impaired by BPL treatment. Although BPL treatment did not totally inhibit the membrane fusion activity even at the highest doses, the FRET experiments showed that this inhibition is a BPL dose-dependent process suggesting that one or more proteins involved in this mechanism have their functions altered by BPL.

### 3.3. Effect of BPL treatment on calcein leakage

HA protein is involved at different levels of the membrane fusion process. The N-terminal fusion peptide of the HA2 subunit undergoes a conformational change triggered by the pH decrease leading to its insertion into the target membrane [10–12,41]. This process was monitored by spectrofluorometric measurement of calcein escape, a small negatively charged fluorescent molecule entrapped in liposomes and self-quenched at high concentration. Its leakage from the internal volume of liposomes was induced by the penetration of viral fusion peptide within the target lipid membrane [42,43]. Fusion peptides perturbing locally the target membrane triggered calcein release from liposomes leading to a strong increase of fluorescence [12]. Native and BPL-treated viruses were incubated at pH 5.1 with liposomes containing entrapped calcein (Fig. 2B). Native and BPL-treated viruses exhibited high calcein leakage activity. Calcein escape was massive for native virus (close to 62%) and in a range of 35% to 45% for all BPL-treated virus (100% corresponding to full dequenched calcein). Calcein leakage was significantly reduced for BPL-treated virus compared to native virus. Following treatment with 2 μM BPL, a leakage of 37% was measured, revealing that the process efficiency was already slowed down at low BPL treatment. For treatments with higher BPL concentrations, we observed that the decrease of molecule leakage was not related to BPL doses, unlike the membrane fusion process. These results suggest that BPL treatment leads to the inactivation of some HA proteins whereas others remain functional. The similarities of the initial kinetic rates suggest that the number of functional HA proteins is not a rate-limiting parameter at the beginning whereas the early onset of the fluorescence leveling off may represent the lack of functional HA species.

### 3.4. Membrane fusion of native and BPL-treated viruses with liposomes observed by cryoTEM and cryoET

At pH 7.4, the overall aspects of BPL-treated and native viruses are very similar. BPL-treated or native viruses were observed in contact with liposomes containing GM3 gangliosides (Fig. S2). At low pH, cryoTEM revealed that the surface of native viruses was fuzzy showing that HA glycoproteins have lost their well defined shape (compared to the rod shape at the neutral pH condition) due to their low pH conformational changes (Fig. 3). Moreover, a large number of liposomes appeared to be in close contact with viruses (Fig. 3A–B). Depending on their deformation at the viral surface, we classified liposomes into three different groups, named intact liposomes (I), liposomes exhibiting a peculiar funnel-like shape (II) and virus-fused liposomes (III) (Fig. 3B). Using cryoET, we were able to get further structural information of liposome groups I and II (Fig. 3C–G). On three extracted Z-slices from the tomogram, enabling the visualization of upper, equatorial and lower part of viruses, liposomes I appeared in close interaction with glycoproteins, while maintaining their spherical shape and membrane continuity (Fig. 3C). Unlike liposomes of group I, the lipid membrane of group II liposomes was disrupted at the contact zone with the virus

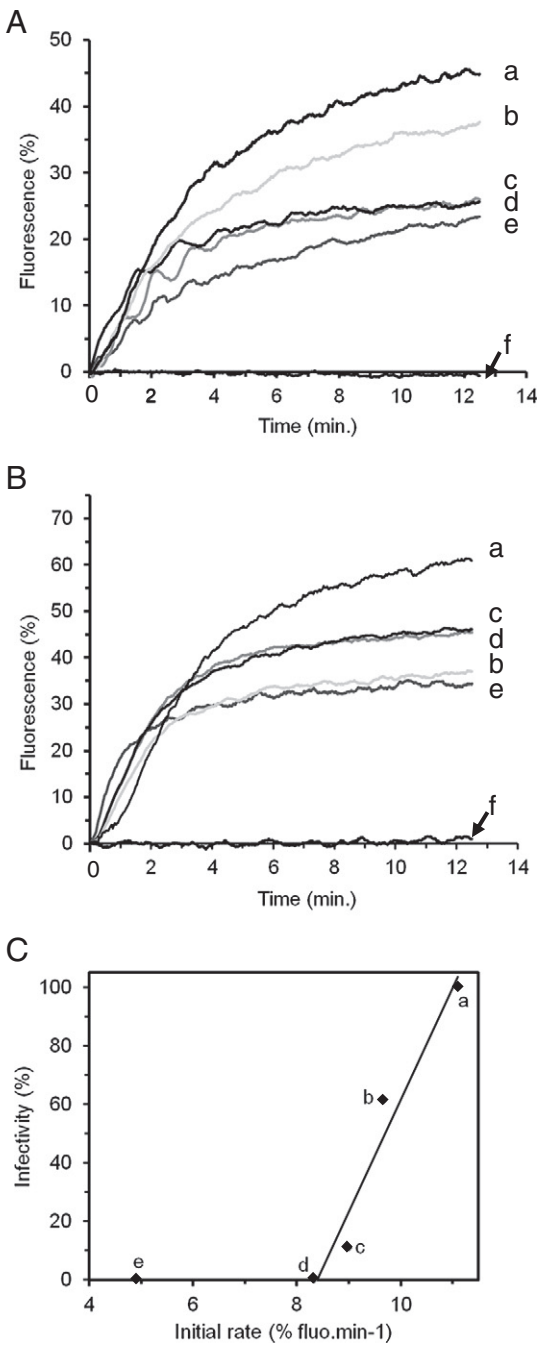


**Fig. 2.** BPL effect on virus membrane fusion and on calcein leakage. A) BPL-treated and native viruses were incubated with [*N*-NBD-PE/*N*-Rh-PE] - labeled liposomes containing GM3 gangliosides. Membrane fusion was measured with a FRET assay for various BPL doses at pH 5.1. B) BPL-treated and native viruses incubated with calcein-loaded GM3 liposomes. Dequenching of fluorescent probes due to calcein leakage arising from HA fusion peptide insertion in target membrane was measured for various BPL doses at pH 5.1 and room temperature. a, b, c, d and e correspond to 0, 2, 20, 250 and 1.000 μM BPL treated virus respectively. As control experiment, native virus incubated with GM3 liposomes at pH 7.4 is presented in f. C) Infectivity versus Initial rate of membrane fusion for the BPL treatment conditions. A linear regression could be fitted within the range of 0 to 250 μM BPL corresponding to 'a' to 'd' in A). 1,000 μM BPL condition ('e' in A)) was excluded from the linear regression.

(arrow Fig. 3C) and formed a 12 nm hole as shown in Fig. 3C (arrow). The zone of this membrane hole interacted with protein densities of the virus which corresponds to a typical fusion intermediate step named "protein pore" according to Lee [15]. Liposomes of group III revealed glycoproteins at the surface of liposomes covering partially the membrane surface, strongly suggesting that such complex structure

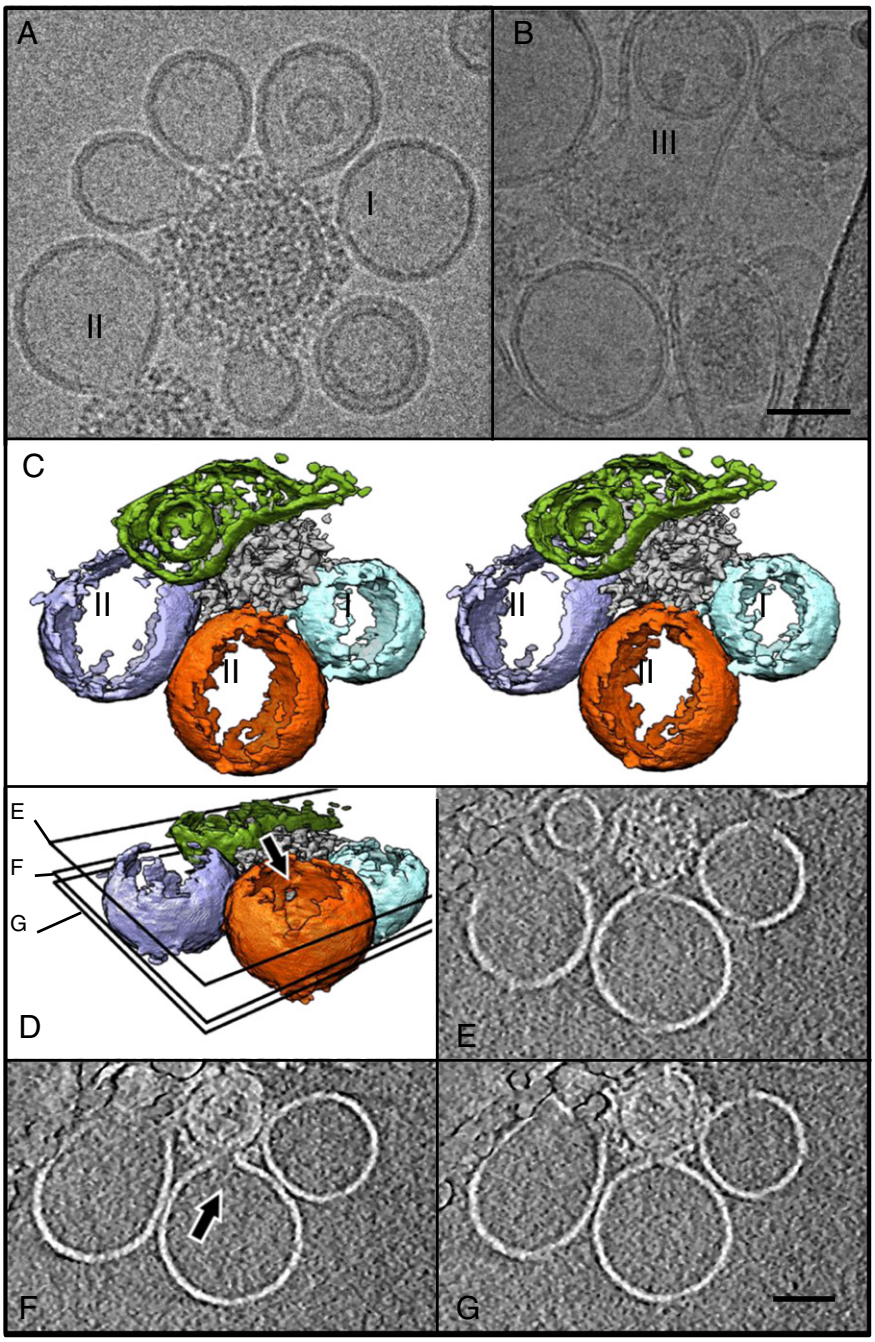


**Fig. 3.** CryoTEM and cryoET of native virus incubated with liposomes at pH 5.1. A) Typical images of native virus interacting with liposomes revealing different steps of viral membrane fusion process correspond to intact liposome interacting with virus (I), ruptured liposome (II), B) typical image of product of viral membrane fusion (III). These steps correspond to early, intermediate and late steps of viral membrane fusion process. C–G). Liposomes I and II analyzed by cryoET. C) Stereoscopic view of isosurface showing liposomes (I and II) colored in green, purple, blue surrounding the virus (gray color). D) Isosurface of tomogram portion and three Z-slices ($Z = 131$ (E), $Z = 92$ (F) and $Z = 80$ (G)) extracted from the tomogram showing liposomes I and II. For the sake of clarity, the contrast was inverted in the tomogram. Note the ruptured lipid membrane II in contact with glycoprotein densities (arrow in F) which forms a 12 nm circular pore (arrow in D). Scale bars are 50 nm.

arose from a complete virus–liposome fusion event. Taken together, cryoTEM images revealed virus–liposome complexes trapped in the early, intermediate and late steps of the viral membrane fusion process.

BPL-treated viruses were observed under the same conditions to assess structural alterations caused by BPL treatment. The same liposome classification was carried out (see Table S2 for liposome distribution) and the most advanced events of viral membrane fusion process were presented in Fig. 5. Viral samples treated with 2 μM BPL interacted with liposomes leading to complete fusion events i.e. liposome (III) (Fig. 4A).

At elevated BPL concentrations the cryoTEM analyses revealed that deformed liposomes (II) were still present. No complete fusion event was encountered, which contrasts somehow the above reported FRET measurements, in which clearly residual fusion events were observed at the same BPL concentration. It may be hypothesized that this level of membrane fusion events seems too low for their observations by cryoTEM and may be a potential cause for these differences. These cryoTEM observations were thus indicative of the efficiency of membrane fusion process and were in good agreement with FRET measurements. All together these results provided evidence that BPL treatment impaired virus fusion in a dose dependent manner (Fig. 4B–D). We have observed that the function of HA molecules is altered. According to leakage measurements, BPL treatment has an effect on

HA molecules by preventing the fusion peptide insertion. But all HA molecules are not concerned by this preclusion. Some HA molecules remained fully functional irrespectively to BPL doses. Thus, the dose-dependent inhibition of membrane fusion should involve another protein than HA. But also, this finding raises the question of whether the membrane inhibition is related to protein modifications.

### 3.5. BPL treatment modified viral assembled proteins

In order to evaluate whether BPL reacts with virus-assembled proteins, mass spectrometry (MS) has been used to monitor protein modification following treatment with 1 mM BPL. After deglycosylation and SDS-PAGE electrophoresis, proteins were submitted to trypsine digestion followed by MALDI-TOF mass spectrometry. Three peptides have been unambiguously identified from HA2 subunit and M1 matrix proteins (Table 1). One molecule of BPL reacted with Lys68 and Lys143 for HA2 subunit and with Glu152, Asp156 or His159 for M1 matrix protein. Interestingly, the targeted Lys68 of HA2 is located within a loop of HA stem core at neutral pH. At low pH this loop adopts a helical structure triggering the exposure of fusion peptide at the coiled coil top [9]. This conformational change might be affected by this BPL modification. For HA1 and vRNP, peptide modifications were not observed. Because MALDI-TOF is not a quantitative method, it is difficult to conclude whether these two proteins remain intact. We have not been able to analyze Neuraminidase and M2 protonophore due to a low number of copies present in the virus. These MS results demonstrated that BPL reacted with viral assembled proteins suggesting that this membrane inhibition would be due to functional blocking of some proteins because of their chemical modification. Inactivation of HA could be caused by the modification of amino acids (Lys68 and 143) of HA2. Membrane fusion being a multistep process involving several proteins, we further explored how the acidification process and M1 dissociation is disturbed by BPL.

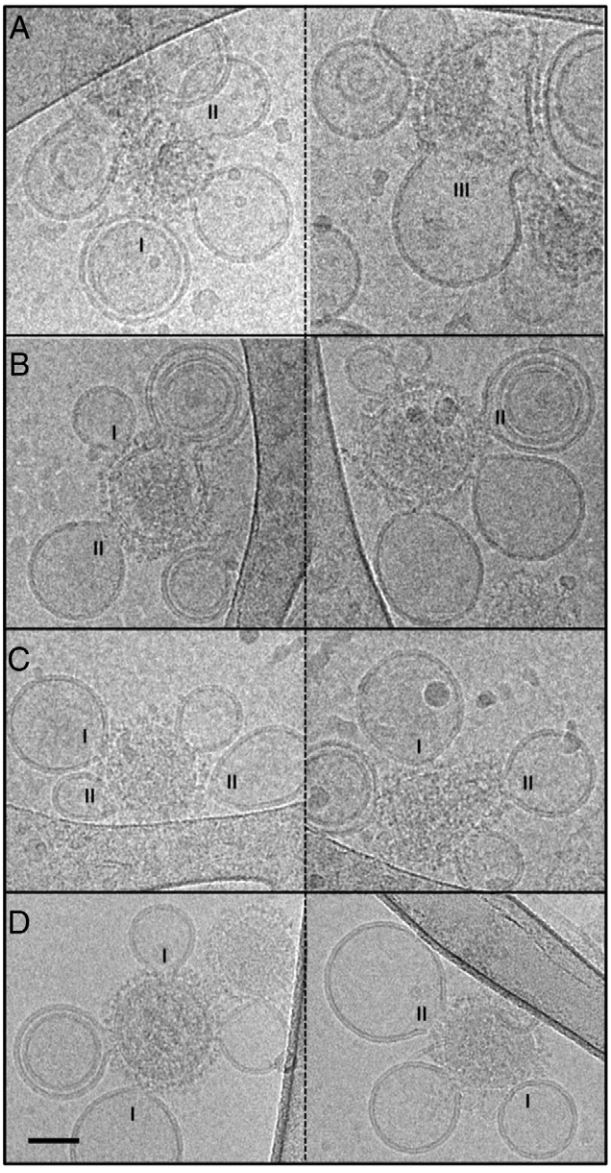


**Fig. 4.** Typical cryoTEM images of BPL-treated virus incubated with liposomes at pH 5.1. A) At 2 μM BPL, liposomes (I), (II) and (III) were observed. B, C) At 20 and 250 μM BPL respectively, only liposomes (I) and (II) were encountered. D) At 1,000 μM BPL, liposomes (I) were present while liposome (II) was scarcely observed. Annotations I to III are described in Fig. 3. Scale bar is 50 nm.

### 3.6. Membrane fusion of native and BPL-treated viruses with liposomes enhanced by addition of monensin

The increase of $H^+$ concentration causes irreversible conformational changes of HA, a prelude to the formation of fusion pore and membrane fusion. Concomitantly, the acidification of the interior of the virus is required for triggering M1-vRNPs dissociation that might facilitate membrane fusion [16,17]. The M2 protonophore is responsible for this $H^+$ internalization. Monensin is a polyether antibiotic that acts as a $Na^+/H^+$ ionophore by forming stable complexes with monovalent cations, able to enhance membrane fusion at 37 °C [34,35]. Virus suspension was incubated with 1 μM monensin for 15 minutes at pH 7 and mixed with liposome suspension at pH 5.1, the FRET kinetics being recorded at 37 °C (Fig. 5A). In the presence of monensin, native virus exhibited a more efficient membrane fusion activity compared to control measurement (Fig. 5A). Initial rates were significantly increased and the fluorescence intensity at the final level was enhanced (from 40% to 53%). These results were in perfect agreement with data reported previously [34,35]. Monensin had a similar effect on virus treated with 1 mM BPL. Membrane fusion activity was superior both in term of intensity and initial rate (Fig. 5A). Monensin enabled the restoration of membrane fusion activity of BPL-treated virus that is dependent on the level of proton influx controlled by M2 channel. Of note, the fusion activity for BPL-treated virus in the presence of monensin did not reach a level comparable to those measured with native virus since BPL also inhibited by the fusion peptide insertion into the target membrane.

CryoTEM of BPL-treated viruses incubated with monensin were carried out under similar conditions (Fig. 5B). Several complete membrane fusion events (liposomes (III)) were encountered and fully confirmed FRET data that monensin has restored the membrane fusion activity of BPL-treated virus. These events resembled those observed with native virus at the same temperature (data not shown). To get further structural details on these fusion events, cryoET was performed on a liposome (III) (Fig. 5C). As a proof of a product of fusion between a virus and a liposome, this liposome (III) contained an internal vesicle genuinely present before virus fusion (Fig. 5C, D). Sequential Z-slices extracted from tomogram, revealed glycoprotein densities distributed unevenly at the surface of the lipid membrane in good concordance with previous observation [44]. These glycoproteins exhibited globular mass linked to the membrane through a thin tail, likely corresponding to HA [45]. The matrix formed a dense structure detached from lipid membrane. As previously observed with filamentous virus [45], the M1 matrix proteins form a compact structure and are not disassembled into individual molecules after fusion. Although it was difficult to identify vRNPs as coiled structures [46], there were small features at the vicinity of the matrix that might correspond to vRNP (shown by white arrow in Fig. 5C).

**Table 1**
List of peptides presenting BPL addition on assembled proteins.

| | $(M+H)^+$ | Sequence | BPL number | Complementary data |
|---|---|---|---|---|
| HA2 | 1806.8 | FHQIE**K**$_{68}$EFSEVEGR | 1 | Induced a miss cleavage (MC) |
| HA2 | 1778.8 | IYH**K**$_{143}$C*DNAC*IGSIR | 1 | MC and modified cysteine |
| M1 | 2923.4 | MGAVTTEVAFGLVC*ATC*$\mathbf{E}_{152}$QIA$\mathbf{D}_{156}$SQ$\mathbf{H}_{159}$R | 1 | Modified cysteine |

Peptide sequence coverage was 73% for NP, 33% for HA1, 49% for HA2 and 80% for M1 proteins.
* modified cysteine.

### *3.7. Membrane fusion with liposomes of BPL-treated virus was not affected by addition of amantadine unlike native virus*

Monensin experiments suggested that the acidification process of the viral internal compartment was still a parameter of importance for membrane fusion even after BPL treatment. We used amantadine which blocks proton transport through the channel formed by M2 tetramer slowing down membrane fusion activity [34,47–49]. Native and BPL-treated viruses were incubated with increasing amantadine concentrations (10, 50 μg/mL) and FRET assays were performed at pH 5.1 (Fig. 6A). Increasing amantadine concentration progressively inhibited the membrane fusion activity of native virus. For 1 mM BPL-treated virus, the fusion activity was lower than those of native virus treated with amantadine. In addition, incubations of BPL-treated virus with 10 and 50 μg/mL amantadine had no noticeable effect on membrane fusion activity. Addition of amantadine does not reinforce inhibition caused by BPL treatment indicating that M2 channel of BPL-treated virus is not inhibited by amantadine at these concentrations.

## 4. Discussion

Although employed to manufacture many millions of vaccine dosed annually virus inactivation using BPL treatment remains a poorly understood process. BPL was found to react with nucleophilic groups (such as primary or secondary amines) of nucleic acids leading to virus inactivation [19–23]. Molecular studies are required to determine precisely the molecular and structural consequences of BPL action which is an essential prerequisite to rationally optimize industrial scale vaccine production processes.

A major finding of our work consists in the demonstration that viral membrane fusion is altered after BPL treatment. Over a large concentration range from 2 μM to 1 mM BPL, this inhibition is dose-dependent. However the membrane fusion process is not completely abolished even at 1 mM BPL in good concordance with recent observations on H5N1 virus samples inactivated with BPL [18].

The observed decreases of virus infectivity and membrane fusion activity are both BPL dose dependent. FRET experiments show that the

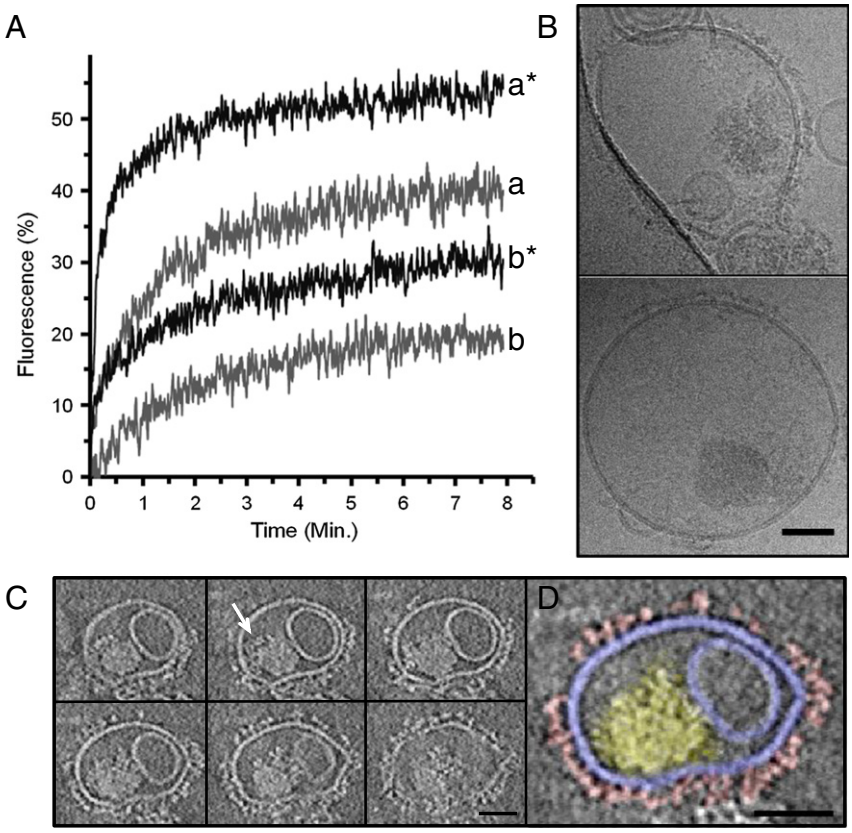


**Fig. 5.** Membrane fusion activity of BPL-treated virus enhanced in the presence of monensin. A) FRET assays monitoring membrane fusion of native (a) and 1000 μM BPL-treated (b) viruses incubated without and with 1 μM monensin (a*, b*) at 37 °C. B) CryoTEM of BPL-treated H3N2 virus in the presence of 1 μM monensin mixed with GM3 liposomes. Liposomes (III) were observed. C, D) Six Z-slices extracted through a liposome (III) tomogram, and an enlarged 7.4 nm slice depicting glycoproteins, lipid membrane, viral matrix manually colored in red, blue and yellow respectively. Elongated features resembling coiled structures (white arrow in C). Scale bars are 50 nm.

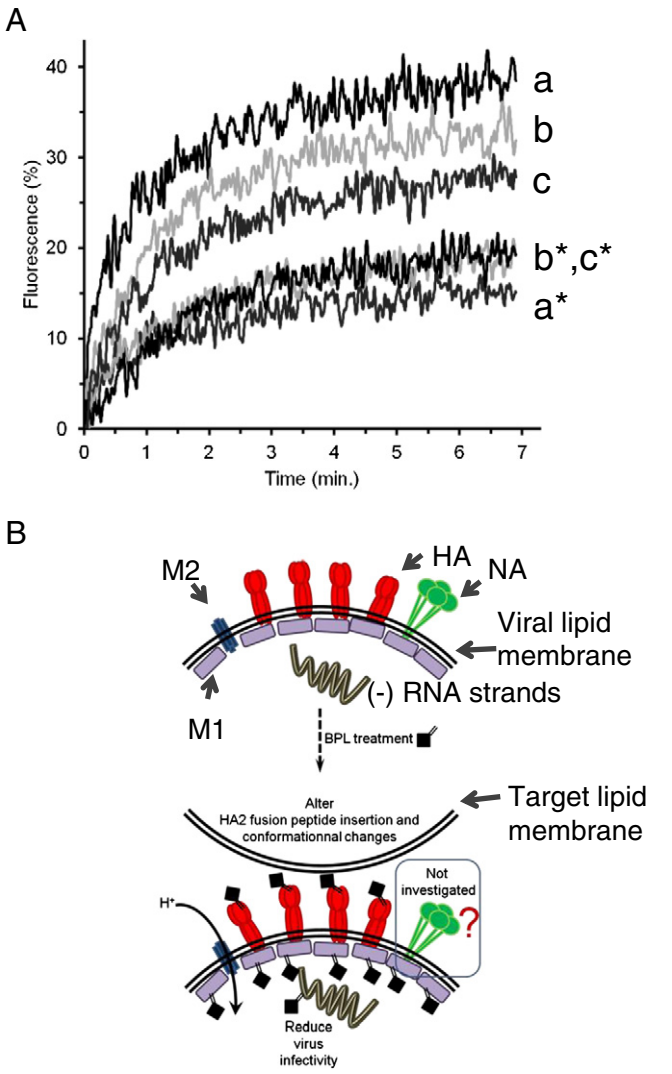


**Fig. 6.** Amantadine effect on membrane fusion activity of native and BPL-treated virus. A) FRET assays monitoring membrane fusion of native virus incubated with 0 (a), 10 (b) and 50 μg/mL amantadine (c) at 37 °C. Likewise, 1000 μM BPL treated virus was incubated with 0 (a*), 10 (b*) and 50 μg/mL amantadine (c*) at 37 °C. B) Scheme of BPL mechanism of action on influenza virus membrane fusion. Virus membrane including HA, NA, M1 and M2 proteins and vRNP have been schematically drawn. Virus inactivation relies on protein modifications involved in membrane fusion process and on nucleic acids modifications.

initial rate of membrane fusion decreases with the increase of BPL dose. On the plot of virus infectivity against the fusion initial rate, a linear regression function was observed between infectivity and initial rate for BPL doses up to 250 μM (Fig. 2C). This direct correlation suggests that at these BPL concentrations (from 2 to 250 μM), loss of infectivity is strictly dependent on membrane fusion inhibition. This analysis reveals that BPL concentrations superior to 250 μM BPL are sufficient for viral inactivation. This also could reflect that virus accessibility for BPL molecules is related to a diffusion gradient across the viral membrane. High BPL concentrations would be required to reach the most buried parts of the virus such as vRNPs. Differences in BPL diffusion within the virus may in part explain the differences reported in the literature concerning the BPL doses required for viral inactivation [22,23]. BPL efficiency may also depend on the corresponding alterations of the viral structures. Our MS data show that among investigated proteins (i.e. HA, M1, vRNP) relatively few amino acids were modified. Even though BPL is reported very reactive on isolated residues [26], the reaction of BPL on whole virus seems much more limited. In the whole virus, proteins are folded into quaternary structures with post-translational modifications such as glycosylation that may restrain the reaction of their nucleophilic groups with BPL. Interestingly, our mass spectrometric analysis reveals that the extent of BPL protein modification of deglycosylated virus is superior to that of glycosylated viruses suggesting a protective role of protein glycosylation (Table S1).

Our data also indicate that BPL could also alter the activity of viral proteins. In terms of virus infectivity, NA (neuraminidase) can yet be excluded from these potential candidates involved in BPL-inactivation mechanism. Indeed, NA is essential for virus budding at the end of the replication process in the host cell but not during the first step of influenza virus infection [8].

The HA1 domain exposes a binding domain to sialic acid while HA2 subunit contains the fusion peptide and undergoes conformational changes triggering membrane fusion. Our MS results showed that HA2 domain was modified by BPL treatment. A modification was depicted on Lys68 of HA2 belonging to a loop which is structured into α helix at low pH to lengthen the coiled coil, the post fusion structure proposed by Bullough et al. [9]. The reduction of calcein release could be also explained by the modification of HA2. This modification prevents the conformational change and subsequently the insertion of fusion peptide in target membrane [12]. Moreover, calcein leakage experiments indicate that native and BPL-treated viruses have similar initial rates suggesting that for HA remaining active, the mechanism triggering the peptide insertion in the target membrane is not modified. Altogether, these results suggest that a low BPL dose was enough for inactivating fusion peptide of HA2. Surprisingly this inactivation did not affect all HA2 proteins since this inhibition is not dose dependent and large amount of HA2 proteins remains active even at higher BPL doses (albeit this amount cannot be determined by fluorescence). Although we do not have clear explanation, it is worth noting that Lys residue can be modified by BPL according to an alkylation or an acylation reaction [26]. The consequence is that acylation of Lys residues results in a neutral moiety at low pH while alkylation results in a cationic secondary amine and an anionic carboxylate. It is not excluded that this difference in Lys modification could lead to two populations of modified HA, having either a full active or an inactive fusion peptide.

In addition to the effect on HA2, there is evidence that BPL treatment affects other proteins involved in the process of membrane fusion. Our MS results showed that M1 matrix was modified by BPL on several amino acids located in the N-terminal domain of the matrix protein. M1 consists of two N- and C-terminal domains which are both involved in the oligomerization of M1. This oligomerization is pH sensitive and is controlled by N-terminal domain which forms oligomer at pH 7.4 and dissociates into monomer at pH 5 [50]. On contrary, C-terminal domain exists as stable dimer which contributes to M1 dimerization. As the BPL modification is located within the pH-sensitive N-terminal domain, it cannot be excluded that this modification could perturb M1 dissociation at low pH, impairing membrane fusion. Amantadine experiments revealed that membrane fusion of BPL-treated virus was not inhibited by amantadine unlike untreated virus (Fig. 6A). Possible explanations could be that amantadine has less affinity for M2 channel after BPL-treatment, or $H^+$ transport has been modified. M2 channel seems also to be affected by BPL treatment. As suggested for vRNP inactivation, the BPL dose effect of membrane fusion activity is probably related to the BPL accessibility suggesting that increasing the dose would modify the most buried proteins. So the measured inhibition of membrane fusion would probably arise from a cumulative inhibition on several proteins rather than on a unique protein. Further MS experiments (i.e. LC-ESI-MS) purposely designed to study M1 and M2 proteins are needed.

## 5. Conclusion

In the present study, we showed that viral membrane fusion is altered after BPL treatment. BPL treatment affects the function of HA by preventing the insertion of its fusion peptide into target membrane,

unveiling in more details the action of BPL (Fig. 6B). It is likely that an additional vRNPs inactivation could provide a cumulative effect allowing the complete abolishment of virus infectivity measured on MDCK cells at high BPL doses. Further experiments are required to study BPL effects on the other components of virus such as the other proteins and vRNPs for a complete understanding of the BPL chemical mechanism of virus inactivation.

## Acknowledgments

We would like to thank Toon Stegmann and Tino Krell for critical reading and comments, Catherine Manin for mass spectrometry expertise, Alain Brisson for equipment support and Sophie Buffin for experimental assistance.

This work was supported by Conseil Regional d'Aquitaine (20071302007) (to OL).

## Appendix A. Supplementary data

Supplementary data to this article can be found online at http://dx.doi.org/10.1016/j.bbamem.2013.09.021.

## References

[1] A. Harris, G. Cardone, D.C. Winkler, J.B. Heymann, M. Brecher, J.M. White, A.C. Steven, Influenza virus pleiomorphy characterized by cryoelectron tomography, Proc. Natl. Acad. Sci. U. S. A. 103 (2006) 19123–19127.
[2] W. Weis, J.H. Brown, S. Cusack, J.C. Paulson, J.J. Skehel, D.C. Wiley, Structure of the influenza virus haemagglutinin complexed with its receptor, sialic acid, Nature 333 (1988) 426–431.
[3] S.C. Harrison, Viral membrane fusion, Nat. Struct. Mol. Biol. 15 (2008) 690–698.
[4] M. Knossow, J.J. Skehel, Variation and infectivity neutralization in influenza, Immunology 119 (2006) 1–7.
[5] J.J. Skehel, D.C. Wiley, Receptor binding and membrane fusion in virus entry: the influenza hemagglutinin, Annu. Rev. Biochem. 69 (2000) 531–569.
[6] T. Stegmann, Membrane fusion mechanisms: the influenza hemagglutinin paradigm and its implications for intracellular fusion, Traffic 1 (2000) 598–604.
[7] I.A. Wilson, J.J. Skehel, D.C. Wiley, Structure of the haemagglutinin membrane glycoprotein of influenza virus at 3 A resolution, Nature 289 (1981) 366–373.
[8] S.J. Gamblin, J.J. Skehel, Influenza hemagglutinin and neuraminidase membrane glycoproteins, J. Biol. Chem. 285 (2010) 28403–28409.
[9] P.A. Bullough, F.M. Hughson, J.J. Skehel, D.C. Wiley, Structure of influenza haemagglutinin at the pH of membrane fusion, Nature 371 (1994) 37–43.
[10] T. Stegmann, J.M. Delfino, F.M. Richards, A. Helenius, The HA2 subunit of influenza hemagglutinin inserts into the target membrane prior to fusion, J. Biol. Chem. 266 (1991) 18404–18410.
[11] M. Tsurudome, R. Glück, R. Graf, R. Falchetto, U. Schaller, J. Brunner, Lipid interactions of the hemagglutinin HA2 NH2-terminal segment during influenza virus-induced membrane fusion, J. Biol. Chem. 267 (1992) 20225–20232.
[12] P. Bonnafous, T. Stegmann, Membrane perturbation and fusion pore formation in influenza hemagglutinin-mediated membrane fusion A new model for fusion, J. Biol. Chem. 275 (2000) 6160–6166.
[13] A.L. Lai, L.K. Tamm, Shallow boomerang-shaped influenza hemagglutinin G13A mutant structure promotes leaky membrane fusion, J. Biol. Chem. 285 (2010) 37467–37475.
[14] L.V. Chernomordik, V.A. Frolov, E. Leikina, P. Bronk, J. Zimmerberg, The pathway of membrane fusion catalyzed by influenza hemagglutinin: restriction of lipids, hemifusion, and lipidic fusion pore formation, J. Cell Biol. 140 (1998) 1369–1382.
[15] K.K. Lee, Architecture of a nascent viral fusion pore, EMBO J. 29 (2010) 1299–1311.
[16] K. Martin, A. Helenius, Nuclear transport of influenza virus ribonucleoproteins: the viral matrix protein (M1) promotes export and inhibits import, Cell 67 (1991) 117–130.
[17] M. Lakadamyali, M.J. Rust, X. Zhuang, Endocytosis of influenza viruses, Microbes Infect. 6 (2004) 929–936.
[18] N. Budimir, A. Huckriede, T. Meijerhof, L. Boon, E. Gostick, D.A. Price, J. Wilschut, A. de Haan, Induction of heterosubtypic cross-protection against influenza by a whole inactivated virus vaccine: the role of viral membrane fusion activity, PLoS ONE 7 (2012) e30898.
[19] E.I. Budowsky, E.A. Friedman, N.V. Zheleznova, Principles of selective inactivation of viral genome VII. Some peculiarities in determination of viral suspension infectivity during inactivation by chemical agents, Vaccine 9 (1991) 473–476.
[20] E.I. Budowsky, E.A. Friedman, N.V. Zheleznova, F.S. Noskov, Principles of selective inactivation of viral genome VI Inactivation of the infectivity of the influenza virus by the action of beta-propiolactone, Vaccine 9 (1991) 398–402.
[21] E.I. Budowsky, Y.A. Smirnov, S.F. Shenderovich, Principles of selective inactivation of viral genome. VIII. The influence of beta-propiolactone on immunogenic and protective activities of influenza virus, Vaccine 11 (1993) 343–348.
[22] P. Perrin, S. Morgeaux, Inactivation of DNA by beta-propiolactone, Biologicals 23 (1995) 207–211.
[23] A. Scheidler, K. Rokos, T. Reuter, R. Ebermann, G. Pauli, Inactivation of viruses by beta-propiolactone in human cryo poor plasma and IgG concentrates, Biologicals 26 (1998) 135–144.
[24] P.D. Bartlett, G. Small, beta-Propiolactone IX the kinetics of attack by nucleophilic reagents upon the alcoholic carbon of p-propiolactone, J. Am. Chem. Soc. 72 (1950) 4867–4869.
[25] M.A. Taubman, M.Z. Atassi, Reaction of beta-propiolactone with amino acids and its specificity for methionine, Biochem. J. 106 (1968) 829–834.
[26] J.P. Uittenbogaard, B. Zomer, P. Hoogerhout, B. Metz, Reactions of beta-propiolactone with nucleobase analogues, nucleosides, and peptides: implications for the inactivation of viruses, J. Biol. Chem. 286 (2011) 36198–36214.
[27] M. Shafique, J. Wilschut, A. de Haan, Induction of mucosal and systemic immunity against respiratory syncytial virus by inactivated virus supplemented with TLR9 and NOD2 ligands, Vaccine 30 (2012) 597–606.
[28] C.J.F. Böttcher, C.M. Van gent, C. Pries, A rapid and sensitive sub-micro phosphorus determination, Anal. Chim. Acta. 24 (1961) 203–204.
[29] B. Desbat, E. Lancelot, T. Krell, M.-C. Nicolaï, F. Vogel, M. Chevalier, F. Ronzon, Effect of the β-propiolactone treatment on the adsorption and fusion of influenza A/Brisbane/59/2007 and A/New Caledonia/20/1999 Virus H1N1 on a dimyristoylphosphatidylcholine/Ganglioside GM3 mixed phospholipids monolayer at the air–water interface, Langmuir 27 (2011) 13675–13683.
[30] A. Roberts, E.W. Lamirande, L. Vogel, B. Baras, G. Goossens, I. Knott, J. Chen, J.M. Ward, V. Vassilev, K. Subbarao, Immunogenicity and protective efficacy in mice and hamsters of a β-propiolactone inactivated whole virus SARS-CoV vaccine, Viral Immunol. 23 (2010) 509–519.
[31] D.J. Finney, Statistical method in biological assay, 1952.
[32] D.K. Struck, D. Hoekstra, R.E. Pagano, Use of resonance energy transfer to monitor membrane fusion, Biochemistry 20 (1981) 4093–4099.
[33] T. Stegmann, D. Hoekstra, G. Scherphof, J. Wilschut, Kinetics of pH-dependent fusion between influenza virus and liposomes, Biochemistry 24 (1985) 3107–3113.
[34] R. Bron, A.P. Kendal, H.D. Klenk, J. Wilschut, Role of the M2 protein in influenza virus membrane fusion: effects of amantadine and monensin on fusion kinetics, Virology 195 (1993) 808–811.
[35] S.A. Wharton, R.B. Belshe, J.J. Skehel, A.J. Hay, Role of virion M2 protein in influenza virus uncoating: specific reduction in the rate of membrane fusion between virus and liposomes by amantadine, J. Gen. Virol. 75 (Pt 4) (1994) 945–948.
[36] Q.S. Zheng, M.B. Braunfeld, J.W. Sedat, D.A. Agard, An improved strategy for automated electron microscopic tomography, J. Struct. Biol. 147 (2004) 91–101.
[37] D.N. Mastronarde, Dual-axis tomography: an approach with alignment methods that preserve resolution, J. Struct. Biol. 120 (1997) 343–352.
[38] H. Chen, D.D. Hughes, T.A. Chan, J.W. Sedat, D.A. Agard, IVE (Image Visualization Environment): a software platform for all three-dimensional microscopy applications, J. Struct. Biol. 116 (1996) 56–60.
[39] E.F. Pettersen, T.D. Goddard, C.C. Huang, G.S. Couch, D.M. Greenblatt, E.C. Meng, T.E. Ferrin, UCSF Chimera—a visualization system for exploratory research and analysis, J. Comput. Chem. 25 (2004) 1605–1612.
[40] T. Stegmann, J.M. White, A. Helenius, Intermediates in influenza induced membrane fusion, EMBO J. 9 (1990) 4231–4241.
[41] T. Shangguan, D. Alford, J. Bentz, Influenza–virus–liposome lipid mixing is leaky and largely insensitive to the material properties of the target membrane, Biochemistry 35 (1996) 4956–4965.
[42] R. Jiricek, G. Schwarz, T. Stegmann, Pores formed by influenza hemagglutinin, Biochim. Biophys. Acta 1330 (1997) 17–28.
[43] Y. Li, X. Han, A.L. Lai, J.H. Bushweller, D.S. Cafiso, L.K. Tamm, Membrane structures of the hemifusion-inducing fusion peptide mutant G1S and the fusion-blocking mutant G1V of influenza virus hemagglutinin suggest a mechanism for pore opening in membrane fusion, J. Virol. 79 (2005) 12065–12076.
[44] P. Bonnafous, M. Perrault, O. Le Bihan, B. Bartosch, D. Lavillette, F. Penin, O. Lambert, E.-I. Pécheur, Characterization of hepatitis C virus pseudoparticles by cryo-transmission electron microscopy using functionalized magnetic nanobeads, J. Gen. Virol. 91 (2010) 1919–1930.
[45] L.J. Calder, S. Wasilewski, J.A. Berriman, P.B. Rosenthal, Structural organization of a filamentous influenza A virus, Proc. Natl. Acad. Sci. U. S. A. 107 (2010) 10685–10690.
[46] T. Noda, H. Sagara, A. Yen, A. Takada, H. Kida, R.H. Cheng, Y. Kawaoka, Architecture of ribonucleoprotein complexes in influenza A virus particles, Nature 439 (2006) 490–492.
[47] S.D. Cady, K. Schmidt-Rohr, J. Wang, C.S. Soto, W.F. Degrado, M. Hong, Structure of the amantadine binding site of influenza M2 proton channels in lipid bilayers, Nature 463 (2010) 689–692.
[48] M. Sharma, C. Li, D.D. Busath, H.-X. Zhou, T.A. Cross, Drug sensitivity, drug-resistant mutations, and structures of three conductance domains of viral porins, Biochim. Biophys. Acta 1808 (2011) 538–546.
[49] M. Sharma, M. Yi, H. Dong, H. Qin, E. Peterson, D.D. Busath, H.-X. Zhou, T.A. Cross, Insight into the mechanism of the influenza A proton channel from a structure in a lipid bilayer, Science 330 (2010) 509–512.
[50] K. Zhang, Z. Wang, X. Liu, C. Yin, Z. Basit, B. Xia, W. Liu, Dissection of influenza A virus M1 protein: pH-dependent oligomerization of N-terminal domain and dimerization of C-terminal domain, PLoS ONE 7 (2012) e37786.